

See discussions, stats, and author profiles for this publication at: <https://www.researchgate.net/publication/8133620>

Polymerizable Bis(2-ethylhexyl)sulfosuccinate: Application in Microemulsion Polymerization

ARTICLE *in* LANGMUIR · JANUARY 2005

Impact Factor: 4.46 · DOI: 10.1021/la0489357 · Source: PubMed

CITATIONS

6

READS

51

4 AUTHORS, INCLUDING:



John Texter

Eastern Michigan University

232 PUBLICATIONS 2,218 CITATIONS

SEE PROFILE

Polymerizable Bis(2-ethylhexyl)sulfosuccinate: Application in Microemulsion Polymerization

John Texter,^{*,†} Liehui Ge,[†] Thomas H. Mourey,[‡] and Trevor G. Bryan[‡]

School of Engineering Technology, Eastern Michigan University, Ypsilanti, Michigan 48197,
and Eastman Kodak Company, Rochester, New York 14650-2136

Received April 29, 2004. In Final Form: October 25, 2004

A hygroscopic and polymerizable salt ([2-methacryloyloxy]ethyl trimethylammonium chloride) is used to ion exchange the sodium ion in AOT (bis[2-ethylhexyl]sulfosuccinate, sodium salt) to produce a polymerizable form of AOT, MDOS ([2-methacryloyloxy]ethyl trimethylammonium bis[2-ethylhexyl]sulfosuccinate). A partial ternary phase diagram of water, MDOS, and methyl methacrylate (MMA) was determined at room temperature (22 ± 1 °C). A relatively large L_2 domain is obtained, but this domain is smaller than that obtained with AOT. Microemulsion polymerization in this domain at 70 °C, using AIBN (azoisobutyronitrile) as an initiator, produces an optically clear copolymer solid domain nearly as large as the L_2 domain. This interesting behavior contrasts with similar studies of Pavel and Mackay [*Langmuir* **2000**, *16*, 8528] using a polymerizable surfactant DDAMA (didecyltrimethylammonium methacrylate) that produced a much larger L_2 domain than MDOS but yielded a much smaller optically clear domain after thermally initiated polymerization. Thermogravimetric analysis indicates that optically clear composites obtained at an MDOS/MMA weight ratio of 1:4 and containing 5% water (w/w; weight % water in microemulsion) released the water in a transition commencing around 160 °C and continuing to 250 °C. Thereafter, the thermal decomposition was substantially impeded relative to poly(methyl methacrylate) as a control, which was due to the fire-resistant nature of the MDOS monomer. Molecular weight measurements indicate MDOS/MMA copolymers form substantially higher molecular weights as the proportion of MDOS increases. At a given radius of gyration, higher MDOS-containing copolymers exhibit higher molecular weights, suggesting a more compact structure with increasing MDOS.

Radical chain polymerization in microemulsions¹ has been found useful for producing latexes from oil-in-water microemulsions,^{2–5} hydrogel latexes from reverse microemulsions,^{6,7} and microporous materials from bicontinuous microemulsions.^{8–10} A challenge in all three of these microemulsion systems has been to find reaction conditions and microemulsion formulations and compositions that enable the capture of the nanoscopic length scales present in the respective microemulsions before polymerization.

Some very useful insight was provided by Moumen, Pileni, and Mackay,¹¹ when they demonstrated that nanoscale latexes could be produced in reverse microemulsions of methacrylate when a methacrylate moiety was substituted for halide as a polymerizable counterion

for the didecyltrimethylammonium cation (DDAMA). Kline¹² also showed that a similar exchange of anions to produce cetyltrimethylammonium vinylbenzoate produced wormlike micelles. The cross-sectional length scale could be captured after polymerization of the exterior vinylbenzoate groups. Pavel and Mackay^{13,14} examined DDAMA in the ternary water–DDAMA–methyl methacrylate (MMA) system and demonstrated that optically clear nanocomposite materials could be obtained by thermally initiating polymerization in the L_2 domain of the corresponding microemulsions. These and other studies^{15–18} suggest that nanoscopic length scales can be captured in microemulsions when a significant reacting component is incorporated as part of the surfactant.

We are interested in developing new solid materials via microemulsion polymerization and in learning how to capture nanoscopic length scales during polymerization to preserve highly dispersed droplets and irregular bicontinuous microstructures for various applications. These include chemically active coatings for anticorrosion, antimicrobial, and self-cleansing applications and fire-resistant polymers for films and bulk materials.

AOT (bis[2-ethylhexyl]sulfosuccinate, sodium salt; Aldrich) was ion exchanged with MADQUAT ([2-methacryloyloxy]ethyl trimethylammonium chloride; Aldrich)

* To whom correspondence should be addressed. E-mail: jtexter@emich.edu.

† Eastern Michigan University.

‡ Eastman Kodak Co.

(1) Pavel, F. M. *J. Dispersion Sci. Technol.* **2004**, *25*, 1–16.

(2) Dunn, A. In *Comprehensive Polymer Science: The Synthesis, Characterization, Reactions and Applications of Polymers*, Vol. 4; Eastmond, G. C., Ledwith, A., Russo, S., Sigwalt, P., Eds.; Pergamon: New York, 1989; pp 219–224.

(3) Co, C. C.; Kaler, E. W. In *Reactions and Synthesis in Surfactant Systems*; Texter, J., Ed.; Marcel Dekker: New York, 2001; Chapter 21, pp 455–469.

(4) Fu, X.-A.; Qutubuddin, S. *Langmuir* **2002**, *18*, 5058–5063.

(5) Steytler, D. C.; Gurgel, A.; Ohly, R.; Jung, M.; Heenan, R. K. *Langmuir* **2004**, *20*, 3509–3512.

(6) Barton, J.; Capek, I. *Macromolecules* **2000**, *33*, 5353–5357.

(7) Landfester, K.; Hentze, H.-P. In *Reactions and Synthesis in Surfactant Systems*; Texter, J., Ed.; Marcel Dekker: New York, 2001; Chapter 22, pp 471–499.

(8) Li, T. D.; Gan, L. M.; Chew, C. H.; Teo, W. K.; Gan, L. H. *Langmuir* **1996**, *12*, 5863–5868.

(9) Chew, C. H.; Li, T. D.; Gan, L. H.; Quek, C. H.; Gan, L. M. *Langmuir* **1998**, *14*, 6068–6076.

(10) Challa, V.; Kuta, K.; Lopina, S.; Cheung, H. M.; von Meerwall, E. *Langmuir* **2003**, *19*, 4154–4161.

(11) Moumen, N.; Pileni, M. P.; Mackay, R. A. *Colloids Surf., A* **1999**, *151*, 409.

(12) Kline, S. R. *Langmuir* **1999**, *15*, 2726–2732.

(13) Pavel, F. M.; Mackay, R. M. *Langmuir* **2000**, *16*, 8568–8574.

(14) Pavel, F. M. *Polymer Blends and Polymer/Nanoparticle Composites from Microemulsions*. Thesis, Clarkson University, Potsdam, NY, 2001.

(15) Hammouda, A.; Gulik, T.; Pileni, M. P. *Langmuir* **1995**, *11*, 3656–3659.

(16) Srisiri, W.; Sisson, T. M.; O'Brien, D. F.; McGrath, K. M.; Han, Y.; Gruner, S. M. *J. Am. Chem. Soc.* **1997**, *119*, 4866–4873.

(17) Taleb, A.; Petit, C.; Pileni, M. P. *Chem. Mater.* **1997**, *9*, 950–959.

(18) Lisiecki, I.; Andre, P.; Filankembo, A.; Petit, C.; Tanori, J.; Gulik-Krzywicki, T.; Ninham, B. W.; Pileni, M. P. *J. Phys. Chem. B* **1999**, *103*, 9168–9175.

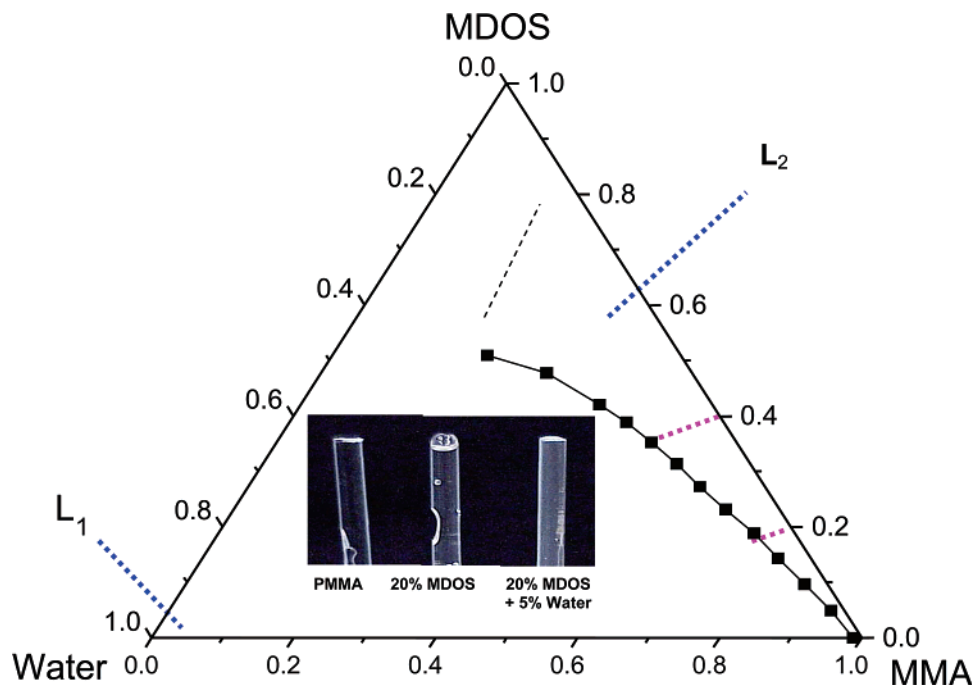
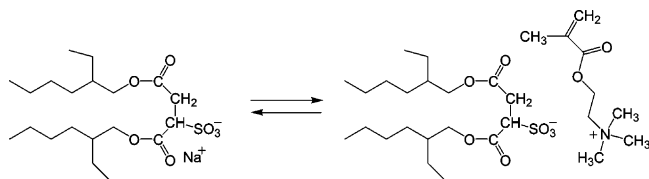


Figure 1. Ternary partial phase diagram at room temperature ($22 \pm 1^\circ\text{C}$) of the water–MDOS–MMA system. Each axis is relative weight fraction. The L_1 domain is too small to see on this scale. The L_2 domain extends past the 75:25 MDOS/MMA ratio, but the upper boundary has not been determined. The lines illustrated within the L_2 domain at 20 and 40% MDOS are loci along which we investigated nanocomposite formation via microemulsion polymerization. The inset illustrates control (PMMA) and poly-MDOS–MMA copolymers obtained at 20:80 MDOS/MMA and at 0% and 5% water (w/w; weight % water in microemulsion) after polymerization at 70°C with 1% AIBN (w/w), relative to total monomer in 5 mm i.d. NMR tubes. This photograph illustrates the very faint turbidity in the copolymer samples. To the naked eye, these copolymer rods appear clear.

Scheme 1. MDOS Formation by Ion Exchange of AOT



in a two-phase ether–water system by repeatedly washing a solution of AOT in ether with aqueous MADQUAT, followed by washing with distilled water, separating the ether phase, evaporating the ether, and drying the product under vacuum at 50°C . Chemical analysis indicated the product had only trace residual sodium-ion content. The nominal structure of the product, (2-methacryloyloxy)ethyl trimethylammonium bis(2-ethylhexyl) sulfosuccinate, which we call MDOS, is shown in Scheme 1. This material has a waxy solid consistency very similar to that of AOT.

A partial ternary phase diagram of water, MDOS, and MMA (Aldrich) at room temperature ($22 \pm 1^\circ\text{C}$) is illustrated in Figure 1. A fairly large compositional area is presented as the L_2 domain. The upper bound to this domain was not found, as compositions 70:30 w/w in MDOS/MMA were the most highly concentrated in MDOS investigated. A definitive but small L_1 domain was also measured and mapped. The size of this L_2 region is about 75% of that obtained with AOT, up to the 50:50 surfactant/MMA ratio. Above this ratio, the AOT L_2 domain is much larger than the one illustrated here for MDOS.

Also illustrated in Figure 1 are two line segments at 20:80 and 40:60 MDOS/MMA. These segments denote loci of microemulsion polymerization. AIBN (azoisobutyronitrile) was used as the thermal initiator. It was used at 1% of total monomer and was dissolved in the MMA. Reverse microemulsions for polymerization were formulated with

no water and with 5% w/w added water and were placed in 5 mm inner diameter NMR tubes immersed in an oil bath at 70°C . After 4 h, the optically clear rods were removed from the tubes (by breaking the tubes) and were seen to be essentially clear and transparent. The rods so obtained for two of these compositions are illustrated in the inset in Figure 1, along with a PMMA (poly(methyl methacrylate)) control. The photography was performed to highlight the very slight turbidity present in the MDOS samples. The appearance of translucency and opacity in similar rods derived from water/AOT/MMA reverse microemulsions by microemulsion polymerizations was shown to be due to microphase separation between the surfactant, AOT, and the PMMA. Scanning electron microscopy (SEM) studies show that at moderate surfactant loading (15% w/w) the AOT formed spheroidal vesicles ($5\text{--}10\ \mu\text{m}$ in diameter) in a continuous PMMA phase and at higher AOT (30% w/w) a more exotic inverse structure was obtained. These preliminary SEM results were kindly provided by Professor Renate Hiesgen and Dr. Jürgen Kraut. Examination of the phase diagram of the water/MDOS binary system shows that the first multiphase region formed past the solubility limit of MDOS in water is a coexistence domain composed of a (lamellar) vesicle phase and an aqueous MDOS micellar phase. This behavior is completely analogous to that seen in the water/AOT system.^{19,20}

Thermal stability using a thermogravimetric analyzer (TA Instruments model SDT 2960 simultaneous DTA-TGA) was examined in air from room temperature to 600°C with a 10°C per min heating rate. Results for the compositions illustrated in the inset to Figure 1 are illustrated in Figure 2. Overall, the MDOS/MMA copoly-

(19) Rogers, J.; Winsor, P. A. *J. Colloid Interface Sci.* **1969**, *30*, 247–257.

(20) Petrov, P. G.; Ahir, S. V.; Terentjev, E. M. *Langmuir* **2002**, *18*, 9133–9139.

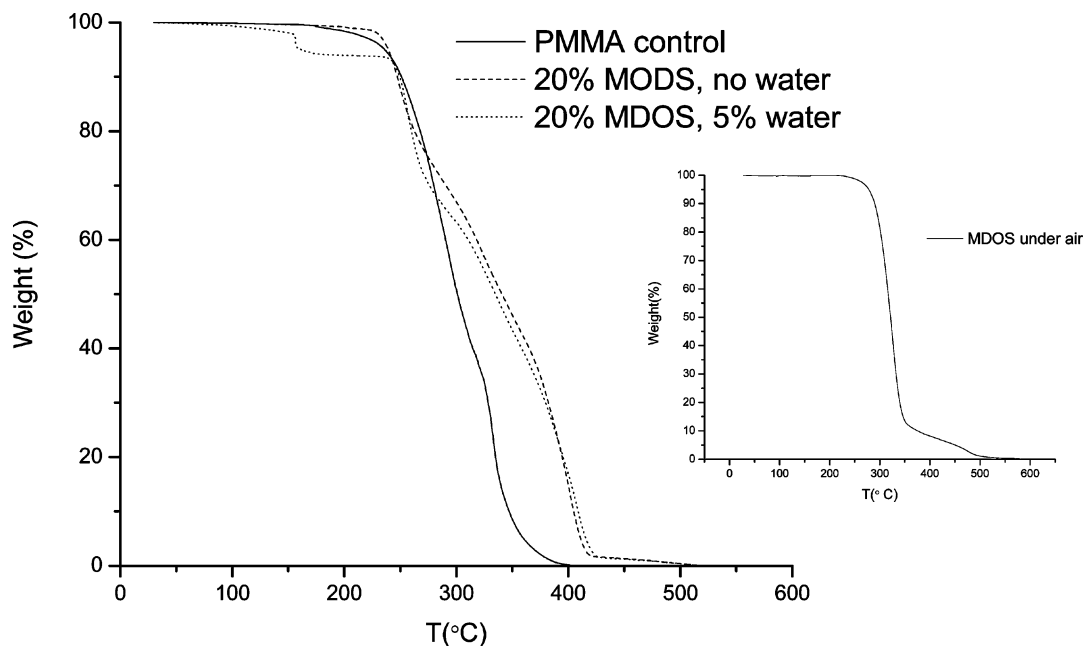
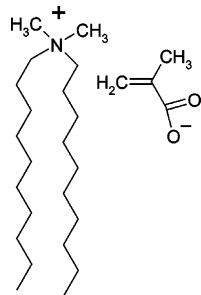


Figure 2. Thermogravimetric analysis of control (PMMA) and copolymer (20/80 MDOS/MMA with and without 5% w/w water) samples illustrated in Figure 1, along with an MDOS control (inset).

Chart 1. DDAM



mers track the PMMA curve to about 260 °C. Above this temperature, the MDOS/MMA copolymers are thermally more robust. The last 70% (of the copolymer) requires over 60 °C higher activation for decomposition. The inset illustrates the decomposition of MDOS, where it is seen that it decomposes over the 300–350 °C range. The last 10–12% of MDOS requires a further 150 °C of activation (350–500 °C), and this remnant is clearly seen in the main part of the figure and corresponds to the last 2–3% loss over the 410–510 °C interval. The sample containing 5% w/w water released the water in a transition, commencing around 160 °C and continuing to about 260 °C. Thereafter, the thermal decomposition was substantially impeded, relative to PMMA as a control, which was due to the intrinsic thermal robustness of the MDOS monomer.

Earlier studies^{13,15} have shown that the surfactant DDAMA (Chart 1) has been effective in capturing nanoscopic length scales in microemulsion polymerization. Pavel and Mackay used this surfactant in the water–DDAMA–MMA ternary system and reported a quite large L_2 domain (compared to what we report in Figure 1). They also carried out thermally initiated (50 °C with benzoyl peroxide as initiator) polymerizations in this domain and reported obtaining optically clear nanocomposites for the domain illustrated in Figure 3 (see Figure 6.22 on page 222 in ref 14).^{13,14} Without water, Pavel also reported that clear polymer phases were obtained up to 35% DDAMA.¹⁴ We also examined similar polymerization behavior and found a considerably larger “optically clear” domain after polymerization, even though the starting L_2 domain in

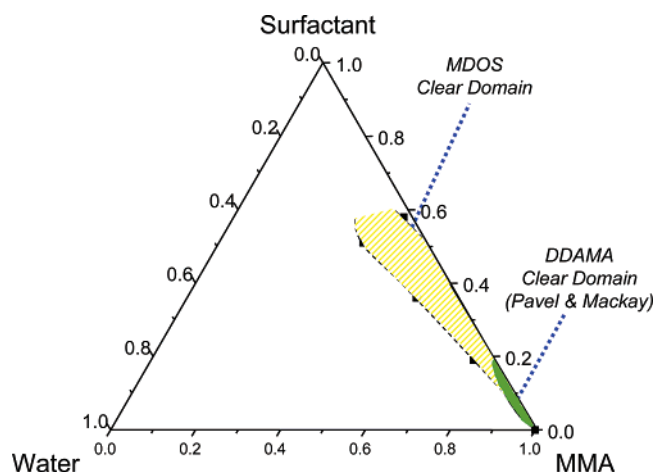


Figure 3. Ternary phase diagram showing the boundaries within the L_2 domain of Figure 1 which resulted after polymerization in clear copolymer nanocomposite domains. Also shown is a similar boundary or map of reverse microemulsion composition with the DDAMA surfactant that yielded clear domains after polymerization, as reported by Pavel [ref 14; see Figure 6.22 on p 222].

our system is smaller. Nearly the entire L_2 domain in this MDOS system yields optically clear nanocomposite after thermally initiated polymerization. The optically clear domain boundary for our system illustrated in Figure 3 was obtained by titration along MDOS/MMA weight ratios of 0.6, 0.4, and 0.2. That is to say that water was titrated into microemulsions of a given MDOS/MMA ratio, along a line segment connecting that ratio on the surfactant–MMA axis and the water corner in the ternary diagram. Increasing amounts of water were added to each of these nonaqueous microemulsions, and then AIBN-initiated polymerization was done at 70 °C. The boundary points are interpolated between the last optically clear composition and the closest “translucent” composition. The uncertainty in these boundary points is less than 0.5% (w/w) water. Note that optical transparency is lost even in the water-free microemulsions at an AOT/MMA ratio

of 0.6, and a small amount of water must be added to obtain transparency in the resulting polymerized composite.

While this L_2 phase domain was articulated at 22 ± 1 °C, our thermally initiated bulk polymerizations were done at 70 °C. While we never saw turbidity form upon placement of our polymerizing microemulsions into the oil bath until a suitable induction time for initiation had passed, a referee suggested we verify the L_2 domain boundary at the temperature of polymerization. We found that the L_2 domain *expands* upon heating to 70 °C. At 0, 0.2, 0.4, 0.5, and 0.6 MDOS/MMA ratios, the L_2 boundary moves toward the water corner by 3, 2, 2, 1.5, and 1% w/w water, respectively.

Transmission electron microscopy (TEM) studies by Pavel and Mackay in the water/DDAMA/MMA system also showed that transparency maintained after polymerization was a result of having only nanoscale aggregates.^{13,14} They found in thin cross-sections that 15–20 nm aggregates were visible, and they hypothesized that these aggregates were predominately polymerized DDAMA, with some MMA incorporation likely. The “continuous” phase after polymerization between such aggregates was predominately PMMA with some DDAMA incorporated. Molecular weight distributions were not reported. We associate the maintenance of transparency after polymerization in our water/MDOS/MMA system with the absence of microphase separation of polymer, surfactant, and water. While microphase separation might occur without turbidity or pronounced increases in light scattering if the indices of refraction of the separated phases were matched, our titration data upon which the clear–turbid boundaries in Figure 3 are based illustrate that very significant changes in scattering occur over very short composition intervals. MDOS and AOT have the same anionic tail group, and both form lamellar liquid crystalline phases. Turbidity in similar water/AOT/MMA microemulsion bulk polymerization systems has been unequivocally assigned to surfactant phase separation on 5–20 μm and larger length scales (forming vesicular–lamellar and more complex structures) on the basis of the preliminary SEM studies by Dr. Kraut and Professor Hiesgen mentioned above. We therefore believe that any microphase separation that occurs results in aggregates such as those reported by Pavel and Mackay, which are of a length scale too small to provide other than Tyndall scattering (e.g., <50 nm). We cannot prove that the same nanostructure present prior to polymerization, such as the particular shape and diameter of surfactant aggregates, has been maintained after polymerization, and it is likely that any “nanophase separation” that occurs, such as the aggregates reported by Pavel and Mackay, produces droplets that are larger than the starting reverse microemulsion droplets. Small-angle neutron scattering (SANS) and/or small-angle X-ray scattering (SAXS) studies with appropriate contrast enhancement will be needed to quantitatively judge to what extent nano-length scales persist after polymerization.

Molecular weight analysis of MDOS/MMA copolymers was done using 1,1,1,3,3,3-hexafluoro-2-propanol (HFIP) because more convenient size-exclusion chromatography (SEC) solvents proved unsuitable. The HFIP was modified to be 0.01 M in tetraethylammonium nitrate, as previously recommended.²¹ Various molecular weight results are illustrated in Table 1 and in Figure 4.

The best number-average molecular weight values come from SEC–viscometry detection and universal calibration.

(21) Mourey, T. H.; Bryan, T. G. *J. Chromatogr. A* **2003**, *36*, 2674–2679.

Table 1. Molecular Weight Moments and Polydispersity of PMMA Control and of MDOS–MMA Copolymers Obtained for Varying MDOS/MMA Monomer Weight Ratios in the Absence of Added Water

polymer	M_n^a	M_w^b	M_z^b	M_w/M_n
PMMA	96 350	533 500	1 230 000	5.5
10:90 MDOS/MMA	123 000	655 000	1 420 000	5.3
20:80 MDOS/MMA	143 000	1 045 000	2 235 000	7.3
30:70 MDOS/MMA	191 500	1 080 000	2 275 000	5.6
40:60 MDOS/MMA	210 500	1 290 000	2 565 000	6.1
50:50 MDOS/MMA	300 000	1 810 000	3 265 000	6.0
60:40 MDOS/MMA	413 000	1 715 000	3 215 000	4.2

^a Viscometry detection and universal calibration. ^b Two-angle light scattering detection.

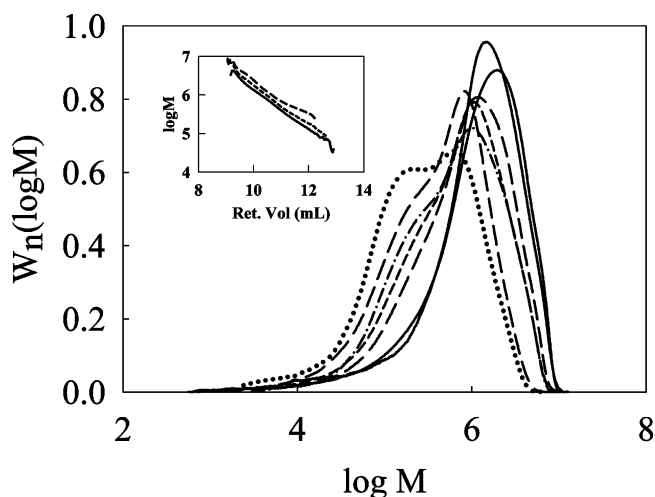


Figure 4. Molecular weight distributions obtained for PMMA control (dot) and copolymer MDOS/MMA samples obtained from water-free solutions of MDOS in MMA, with MDOS contents of 10% (long dash), 20% (dash–dot), 30% (short dash), 40% (dash–dot–dot–dash), 50% (solid), and 60% (medium dash). The inset illustrates molecular weight as a function of retention volume (hydrodynamic size) for PMMA control (solid), 30% (short dash), and 60% (long dash) MDOS.

The viscometer is more sensitive than light scattering detection to the smallest polymer molecules, and the smallest polymer molecules have the greatest influence on M_n . The light scattering detector is best for measuring the weight-average and z -average molecular weights because some of the molecules are too large for the SEC column set and fall outside of the universal calibration curve. The radius of gyration (z -average) is from light scattering, and the intrinsic viscosity was measured by a viscometry detector. All of the “best” values from the different detection methods are summarized in Table 1.

The molecular weight distributions overlaid in Figure 4 indicate that the distributions increase to higher masses as more MDOS comonomer is incorporated. The regions beyond 10^6 are distorted for several reasons, and it is difficult to make quantitative comparisons of distribution shapes. The distortions will likely bias the weight-average and z -average molecular weight averages toward lower values. The inset in Figure 4 shows the 0%, 30%, and 60% MDOS/MMA copolymer samples plotted as $\log M$ versus retention volume. Molecules at the same retention volume have the same hydrodynamic size. These results suggest that the increase in mass with increasing MDOS content for equivalent size molecules is a result of the high mass of the MDOS monomer compared to MMA, although there could be changes in conformation as well; and high-MDOS-content chains may be more compact (globular) in this polar HFIP eluant than 100% PMMA. The bis(2-ethyl-

Table 2. Molecular Weight Moments and Polydispersity of MDOS–MMA Copolymers Obtained for Varying MDOS/MMA Monomer Weight Ratios in the Presence of Added Water

copolymer	M_n^a	M_w^b	M_z^b	M_w/M_n
20:80 MDOS/MMA, 5% water	92 400	676 000	1 170 000	7.3
30:70 MDOS/MMA, 8% water	173 000	638 000	1 050 000	3.7
40:60 MDOS/MMA, 10% water	166 000	713 000	1 170 000	4.3
50:50 MDOS/MMA, 18% water	162 000	726 000	1 230 000	4.5
60:40 MDOS/MMA, 15% water	537 000	1 850 000	3 200 000	3.4

^a Viscometry detection and universal calibration. ^b Two-angle light scattering detection.

hexyl)sulfosuccinate counterion would be expected to induce clustering and intrachain micellization and is consistent with compaction.

Pronounced bimodality in the differential weight-average distributions is exhibited by the PMMA control and by many of the MDOS/MMA copolymers. The PMMA control bimodality appears to be very similar to other reported examples of *bulk* PMMA polymerization.^{22–24} The predominance of the larger molecular weight mode has been ascribed to the gel effect, wherein gelation slows motion of large chains and chain growth proceeds under monomer diffusion control. Ultimately monomer diffusion becomes significantly retarded, and the glass effect sets in, where many shorter length chains are formed during the latest stages of bulk polymerization.

Table 2 illustrates effects of incorporated water on the molecular weights. The compositions chosen over the 20/80 to 60/40 MDOS/MMA ratio interval have added water contents that correspond to compositions just inside (by 0.5–1.5% w/w) the clear domain boundary in Figure 3. Qualitatively, the curve shapes (not illustrated) of the M_w distributions do not change markedly in any obvious way when compared to the shapes obtained for the same monomer ratios without added water (see Figure 4). There is an unequivocal effect of incorporated water on the various molecular weight averages, however. With the single exception of the 60/40 MDOS/MMA ratio case, the various molecular weight averages with added water are approximately 72%, 54%, and 49% of the M_n , M_w , and M_z values, respectively, obtained in the absence of added water. These decreases in molecular weight with addition

of water suggest water may serve as a chain transfer agent. In the 60/40 MDOS/MMA ratio case, the no water system undergoes some sort of microphase separation during polymerization, during which we believe the surfactant (MDOS) becomes much less uniformly distributed. Reports of water acting as a chain transfer agent are mixed, with reports claiming^{25,26} chain transfer activity and others refuting^{27,28} such activity.

Another very significant change with added water, with the single exception of the 20/80 MDOS/MMA composition, is a dramatic decrease in the polydispersity index (PI), M_w/M_n , in comparison to the no added water compositions. The smaller PI values are reminiscent of values obtained in emulsion polymerization and microemulsion polymerization when the continuous phase is water and latex particles are being produced. The very large PI values obtained in the absence of added water here are most likely a consequence of the sequential gel and glass effects discussed above.

Polymerizable forms of “AOT” such as that illustrated here should prove interesting in various microemulsion and mesophase polymerization scenarios. Because of the very large solubility of AOT in many organic solvents and monomers, we think MDOS may have applicability to many systems. Preparation of MDOS is nominally straightforward by two-phase ion exchange.

Acknowledgment. This work was partially supported by a Graduate Research Assistant appointment to Liehui Ge from Eastern Michigan University. We thank Professor David Gore for his photography. We also thank Professor Rick Laine (University of Michigan) for allowing us to use his thermogravimetric analysis system. Thanks are extended to the referees for their suggestions and questions, which were very useful in improving the manuscript. We also thank Professor Francoise Winnik for her reading of the manuscript and for correcting a structural error in Scheme 1. We especially thank Dr. Jürgen Kraut and Professor Renate Hiesgen of the Fachhochschule Esslingen (Germany) for sharing their preliminary SEM analyses of microphase separation in water/AOT/MMA bulk microemulsion polymerized systems with us. A report on the samples examined by Dr. Kraut and Professor Hiesgen has recently appeared.²⁹

LA0489357

(22) Balke, S. T.; Hamelec, A. E. *J. Appl. Polym. Sci.* **1973**, *17*, 905–929.

(23) Maschio, G.; Scali, C. *Macromol. Chem. Phys.* **1999**, *200*, 1708–1721.

(24) Meneghetti, P.; Qutubuddin, S. *Langmuir* **2004**, *20*, 3424–3430.

(25) Gezy, I.; Nasr, H. I. *Kolorisztikai Ertesito* **1970**, *12*, 136–144.

(26) Kucera, M.; Hladky, E.; Gateva, P. Ch.; Spousta, E.; Majerova, K. *Makromol. Chem.* **1966**, *97*, 156–162.

(27) Bhatytagarttam, B. R.; Nandi, U. *J. Polym. Sci., Polym. Chem. Ed.* **1966**, *4*, 2675–2682.

(28) Bhatytagarttam, B. R.; Nandi, U. *J. Indian Chem. Soc.* **1971**, *48*, 1033–1038.

(29) Ge, L.; Texter, J. *Polym. Bull.* **2004**, *52*, 297–305.